

Noninvasive detection of cardiac amyloidosis using delayed enhanced MDCT: a pilot study

Jean-François Deux · Cristian-Ionut Mihalache · François Legou · Thibaud Damy · Julie Mayer · Stéphane Rappeneau · Violaine Planté-Bordeneuve · Alain Luciani · Hicham Kobeiter · Alain Rahmouni

Received: 25 June 2014 / Revised: 17 January 2015 / Accepted: 30 January 2015 / Published online: 19 February 2015
© European Society of Radiology 2015

Abstract

Objectives To evaluate myocardial enhancement of patients with cardiac amyloidosis (CA) using computed tomography (CT).

Methods Thirteen patients with CA and 11 control patients were examined with first-pass and delayed CT acquisition. A qualitative and quantitative analysis of images was performed. Myocardial attenuation, myocardial signal-to-noise ratio (SNR_{myoc}), blood pool SNR (SNR_{blood}), contrast-to-noise ratio between blood pool and myocardium ($CNR_{blood-myoc}$) and relative attenuation index (RAI) defined as variation of myocardial attenuation between delayed and first-pass acquisitions were calculated.

Results Two false negative cases (15 %) and three false positive cases (27 %) were detected on qualitative analysis. SNR_{myoc} of patients with CA was significantly ($p < 0.05$) lower on first-pass (4.08 ± 1.9) and higher on delayed acquisition

(7.10 ± 2.7) than control patients (6.1 ± 2.2 and 5.03 ± 1.8 , respectively). Myocardial attenuation was higher in CA (121 ± 39 HU) than control patients (81 ± 17 HU) on delayed acquisition. $CNR_{blood-myoc}$ was significantly ($p < 0.05$) lower in CA (1.51 ± 0.7) than control patients (2.85 ± 1.2) on delayed acquisition. The RAI was significantly ($p < 0.05$) higher in CA (0.12 ± 0.25) than in control patients (-0.56 ± 0.21).

Conclusion Dual phase MDCT can detect abnormal myocardial enhancement in patients with CA.

Key points

- CT can detect abnormal first-pass and delayed enhancement in cardiac amyloidosis.
- Measurement of relative myocardial enhancement between acquisitions helps to detect cardiac amyloidosis.
- CT may provide useful data to diagnose cardiac amyloidosis.

J.-F. Deux (✉) · C.-I. Mihalache · F. Legou · J. Mayer · A. Luciani · H. Kobeiter · A. Rahmouni
Cardiac MR Unit, Radiology Department, Henri Mondor Hospital, University Paris Est Créteil, Assistance Publique-Hôpitaux de Paris, 51 av Mal de Lattre de Tassigny, 94000 Créteil, France
e-mail: jean-francois.deux@hmn.aphp.fr

J.-F. Deux
CNRS EAC 4396, Centre de Recherches Chirurgicales, Henri Mondor Hospital, University Paris Est Créteil, Assistance Publique-Hôpitaux de Paris, Créteil, France

J.-F. Deux · T. Damy · J. Mayer · S. Rappeneau · V. Planté-Bordeneuve
Réseau Amylose Mondorien, Henri Mondor Hospital, Créteil, France

T. Damy
Cardiology Department, Henri Mondor Hospital, University Paris Est Créteil, Assistance Publique-Hôpitaux de Paris, Créteil, France

V. Planté-Bordeneuve
Department of Neurophysiology of Neurology, Henri Mondor Hospital, University Paris Est Créteil, Assistance Publique-Hôpitaux de Paris, Créteil, France

Keywords Computed tomography · Amyloidosis · Myocardium · Enhancement · Contrast media

Abbreviations

CA	Cardiac amyloidosis
CNR	Contrast-to-noise ratio
CT	Computed tomography
LGE	Late gadolinium enhancement
MDCT	Multidetector computed tomography
RAI	Relative attenuation index
SNR	Signal-to-noise ratio

Introduction

Amyloidosis is a group of uncommon systemic diseases characterized by the extracellular deposition of insoluble fibrillar amyloid proteins [1]. Cardiac involvement is not uncommon in this disease setting—it is encountered in approximately

50 % of patients with the light-chain amyloidosis (AL) form—and is an adverse prognostic marker [2, 3]. Cardiac MRI is a powerful noninvasive technique to identify cardiac amyloidosis (CA) [4]. Amyloid infiltration results in expansion of the extracellular space and modification of gadolinium distribution kinetics leading to accumulation of contrast medium within the myocardium. Thus, many studies have reported a characteristic global subendocardial or diffuse transmural pattern on late gadolinium enhancement (LGE) MRI sequences [5–8]. Nevertheless, MRI is limited by the inability to image patients with pacemakers or implanted cardioverter-defibrillators.

Cardiac CT is used worldwide to noninvasively assess the anatomy of coronary vessels on first-pass acquisition [9, 10]. In addition, several studies have reported that delayed contrast-enhancement multidetector CT (MDCT) acquisition could provide interesting insights into myocardial viability [11–15], fibrosis [16] or inflammation [17] because the iodinated contrast agent accumulates in damaged myocardial tissue in a similar manner to gadolinium chelates. We hypothesized that cardiac MDCT could detect abnormal myocardial enhancement in patients with CA. We conducted a single-centre prospective study to compare myocardial enhancement in patients with CA with a group of control subjects using both first-pass and delayed contrast-enhanced MDCT acquisitions.

Materials and methods

Patients

The study was approved by our local research ethics committee and each included patient provided written informed consent. From January 2012 through January 2013, all 24 patients with systemic amyloidosis and CA were invited to participate. Exclusion criteria were irregular cardiac rhythm ($n=5$), renal insufficiency ($n=3$) and the usual contraindication to MRI ($n=3$; claustrophobia). Thirteen patients were finally included. All of them had a histologically confirmed systemic amyloidosis: six patients had a transthyretin familial amyloidosis (FAP ATTR), five an AL amyloidosis and two a senile systemic amyloidosis. In all these patients, CA diagnosis was assessed on cardiac MRI that evidenced thickening of the cardiac wall (greater than 12 mm for the left ventricle) and diffuse myocardial enhancement on LGE sequences. An endomyocardial biopsy was performed in eight of the 13 patients (61 %) and pathological analysis confirmed CA in all eight patients. Mean left ventricular ejection fraction (LVEF) of the patients was 56.1 ± 11 % (39–76). In addition, 21 consecutive control patients referred for exploration of atypical chest pain were considered for inclusion. Of these, six were excluded because of potential lesions on the coronary arteries or myocardium due to known cardiovascular disease ($n=3$); arterial hypertension ($n=2$); or diabetes mellitus ($n=1$). The remaining 15 control

patients were included. All the patients with CA and control patients had a normal kidney function.

MDCT examination

MDCT was performed in all the patients with CA 3 ± 2 days after cardiac MRI using a 64-detector CT (HD 750; General Electric, MI, USA). The average heart rate during the acquisition was 63 ± 10 bpm (range, 53–82 bpm). A prospective ECG triggering was used to reduce X-ray exposure. Gantry rotation time was 330 ms and a 64×1.25 -mm-wide detector collimation was used. Tube voltage was 100 kVp and tube current was 400 mA. The first-pass contrast-enhanced acquisition was performed after injection of 1.5 mL/kg of contrast medium (Iomeprol 400; Bracco Imaging, France) flushed by saline. The delayed contrast-enhancement acquisition was performed 5 min after injection using the same parameters. The control patients were explored using the same MDCT protocol. Four control patients were excluded because of atherosclerotic lesions on coronary arteries on first-pass imaging ($n=3$) or suspicion of myocardial infarction on delayed contrast-enhanced images ($n=1$). Images of the remaining 11 patients were analysed. Dose-length product (DLP) was recorded for all patients.

CT image analysis

All images were analysed on a dedicated station (ADW 4.6; General Electric, MI, USA).

Qualitative analysis

All the CT images were anonymously reviewed in consensus by two of the authors (CM and JFD). The reviewers independently evaluated three regions: the left ventricle, the right ventricle and the atria. Each region was ranked between 1 and 3 depending on the likely presence of cardiac amyloidosis (1, normal; 2, doubtful; and 3, positive). Criteria taken into account for the diagnosis of cardiac amyloidosis were abnormal enhancement of the wall of the left ventricle, right ventricle and atria between first-pass and delayed images; a narrowing of contrast between blood and the left ventricle, right ventricle and atria on delayed images; and a thickening of the wall of the left ventricle, right ventricle and atria. A global score was also provided for each patient: normal (1), doubtful (2) or positive (3) regarding the diagnosis of cardiac amyloidosis.

Quantitative analysis

Thickness of septum, lateral, inferior and anterior walls of the left ventricle (LV) were measured for all patients and control subjects on a multiplanar reconstruction of first-pass images performed in the mid-short axis plane of the heart. Endo- and epicardial boundaries of the LV were manually defined for all

the patients with CA and the control patients in all contiguous slices of the first-pass and delayed images by one operator (CM). Mean attenuation (Hounsfield unit, HU) of the LV myocardium was automatically calculated by the station at the end of the contouring on first-pass and delayed images. In addition, regions of interest (ROIs) of at least 20 mm² were

placed in the left ventricular cavity and in the air outside the patient on both sets of images to calculate blood pool attenuation (HU), myocardial signal-to-noise ratio (SNR_{myoc}), blood pool SNR (SNR_{blood}) and contrast-to-noise ratio (CNR) between blood pool and myocardium (CNR_{blood-myoc}), using the following formulae:

- $SNR_{myoc} = \text{mean attenuation of the myocardium} / \text{standard deviation of attenuation of the air}$
- $SNR_{blood} = \text{mean attenuation of the blood} / \text{standard deviation of attenuation of the air}$
- $CNR_{blood-myoc} = (\text{mean attenuation of blood pool} - \text{mean attenuation of the myocardium}) / \text{standard deviation of attenuation of the air}$

Lastly, a relative attenuation index (RAI), defined as the variation of myocardial attenuation between delayed

and first-pass acquisitions, was calculated using the following formula:

$$RAI = \frac{(\text{myocardial attenuation on delayed acquisition} - \text{myocardial attenuation on first-pass acquisition})}{\text{myocardial attenuation on delayed acquisition}}$$

MR image analysis

All LGE MR images acquired in the short axis plane were analysed on a dedicated station (ADW 4.6; General Electric, MI, USA).

Qualitative analysis

As for the CT analysis, all LGE images were anonymously reviewed by the same two authors (CM and JFD). Reviewers evaluated enhancement of the left ventricle, right ventricle and atria and each region ranked from 1 to 3 (1, normal; 2, doubtful; and 3, positive). Criteria taken into account for LGE diagnosis of CA were abnormal enhancement associated with a thickening of the wall of the left ventricle, right ventricle and atria. A global score was also provided for each patient: normal (1), doubtful (2) or positive (3).

Quantitative analysis

Endo- and epicardial boundaries of the LV were manually defined for all the patients with CA in all contiguous slices of the short axis LGE images (CM). Mean signal intensity (SI) of LV myocardium was automatically calculated by the station at the end of the contouring on MR images. In addition, ROIs

of at least 20 mm² were placed in the air outside the patient to calculate myocardial signal-to-noise ratio (SNR_{myoc-MRI}).

Statistical analysis

Continuous variables are expressed as mean ± standard deviation. A non-parametric Mann–Whitney test was used to compare quantitative data because of the low number of subjects. Receiver operating characteristic (ROC) analysis, with corresponding measures of statistical uncertainty (i.e. 95 % confidence intervals), was applied to the RAI. A ROC curve was used to identify the cut-off value of myocardial signal for cardiac involvement. The cut-off for myocardial signal was determined using Youden's test. Sensitivity and specificity were calculated using the thresholds previously defined. Spearman's correlation was performed between myocardial attenuation and wall thickness. Data were considered significant if $p < 0.05$. Analyses were performed using SPSS 16.0 software (SPSS Inc., Chicago, IL).

Results

The characteristics of the patients with CA and the control patients are presented in Table 1. Age and sex ratio were not significantly different between the groups. Mean New York

Table 1 Characteristics of the 13 patients with cardiac amyloidosis and 11 control patients

	Patients with cardiac amyloidosis	Control patients	<i>P</i> value
Age (years)	65±11	61±10	0.3
Men (%)	9 (70)	6 (55)	0.2
NHYA functional class	2.2 (1–4)	1	
Signs of cardiac amyloidosis on EKG ^a	2 (15)	NA	
Medications			
Beta blockers	6 (46)	0 (0)	
ACE inhibitor	5 (38)	0 (0)	
LVEF ^b (%)	56.1±11 (39–76)	NA	
Familial amyloidosis	6 (46)	NA	
AL amyloidosis	5 (38)	NA	
Senile amyloidosis	2 (16)	NA	

Data are mean±SD or number (%)

NA not applicable, ACE angiotensin-converting enzyme, LVEF left ventricular ejection fraction, NYHA New York Heart Association

^a Microvoltage (<5 mm on all leads) or Q waves

^b Measured on cardiac MRI

Heart Association (NYHA) functional class was higher in the patients with CA than in control subjects. Patients with CA were more frequently treated with β -blockers and angiotensin-converting enzyme (ACE) inhibitors than the control subjects. The mean LVEF of patients with CA calculated on MRI was in the normal range.

Qualitative analysis

Among the 13 patients with CA, CT was considered as positive, doubtful or negative in seven (54 %), four (31 %) and two (15 %) patients, respectively. For patients attributed a positive or doubtful ranking, the left ventricle was always found to be involved (i.e. a score of 1 for all 11 patients). The right ventricle was ranked as positive in one (8 %) patient and doubtful in another (8 %). Atria involvement was ranked as positive in two (15 %) patients and doubtful in one (8 %). In the 11 control patients, zero (0 %), three (27 %) and eight (73 %) patients were ranked as positive, doubtful or negative, respectively. As for the patients with CA, all three patients with a doubtful ranking had left ventricular involvement. The right ventricle and atria were normal in all control subjects.

Qualitative analysis of the MR images resulted in a positive ranking for all the patients with CA, and the left ventricle was always involved. The right ventricle was ranked as positive or doubtful in three (23 %) and three (23 %) patients, respectively. The atria were frequently involved: positive or doubtful in eight (61 %) and two (15 %) patients, respectively.

Quantitative analysis

Mean DLP values were 228±94 and 193±65 mGy cm, respectively for the patients with CA and the control patients ($p=0.3$, NS). The patients with CA exhibited significantly higher LV wall thickness than the control patients (Table 2).

On first-pass CT images, the patients with CA exhibited a significantly lower SNR_{myoc} than the control subjects (Table 3). Myocardial attenuation was non-significantly lower in the patients with CA ($p=0.1$). Blood pool attenuation, SNR_{blood} and CNR_{blood-myoc} were in the same range for both groups. On delayed CT images (Table 4), myocardial attenuation and SNR_{myoc} were significantly higher in the patients with CA than in the control patients. Blood pool attenuation and SNR_{blood} were in the same range for both groups and consequently CNR_{blood-myoc} was significantly lower in the patients with CA. The mean value of the RAI was 0.12±0.25 in patients with CA. It was positive in all but two and reflected the increase in myocardial attenuation between first-pass and delayed images. In contrast, all the control patients exhibited a negative value of the RAI (mean value -0.56 ± 0.21) because their myocardial attenuation decreased between first-pass and delayed acquisitions. It was statistically ($p<0.05$) lower than that of the patients with CA. Images of patients with CA and control patients are reported in Figs. 1, 2 and 3.

On quantitative MR images analysis, mean SI and SNR_{myoc-MRI} of patients with CA were 28.4±11 (14–53) and 27.03±24 (6.2–92.4), respectively.

The ROC curve and Youden's test identified an optimal threshold of -0.32 for the relative attenuation index (AUC, 1; 95 % CI [1]; $p=0.0001$) as the best threshold for predicting cardiac involvement on MDCT. Sensitivity and specificity of the -0.32 threshold value to predict cardiac involvement were 100 % and 100 %, respectively. Weak but significant negative correlations were observed between myocardial attenuation measured on first-pass images and anterior wall thickness ($r=-0.46$; $p=0.03$), inferior wall thickness ($r=-0.45$; $p=0.04$), interventricular wall thickness ($r=-0.43$; $p=0.05$) and lateral wall thickness ($r=-0.66$; $p=0.002$). No significant correlation was detected

Table 2 Thickness of the left ventricular wall in the 13 patients with cardiac amyloidosis and in the 11 control patients

	Patients with cardiac amyloidosis	Control patients	<i>P</i> value
Anterior wall thickness (mm)	10.5±3	6.3±1	0.003
Inferior wall thickness (mm)	10.1±3	6.5±1	0.006
Interventricular wall thickness (mm)	16.8±5	10.5±3	0.005
Lateral wall thickness (mm)	11.2±3	7.5±2	0.007

Data are mean±SD

Table 3 Myocardial and blood pool attenuation, SNR_{myoc} , SNR_{blood} and $CNR_{blood-myoc}$ in the 13 patients with cardiac amyloidosis and in the 11 control patients on first-pass CT images

	Patients with cardiac amyloidosis	Control patients	<i>P</i> value
Myocardial attenuation (HU)	104±29	128±37	0.1
Blood pool attenuation (HU)	561±172	534±208	0.7
SNR_{myoc}	4.08±1.9	6.1±2.2	0.04
SNR_{blood}	21.9±10	25.2±11	0.5
$CNR_{blood-myoc}$	17.9±9	19.0±9	0.8

Data are mean±SD

HU Hounsfield unit

between myocardial attenuation measured on delayed enhanced images and wall thickness. No significant correlation was found between MR parameters reflecting myocardium signal on LGE images (SI and $SNR_{myoc-MRI}$) and CT parameters. LVEF was weakly correlated with $CNR_{blood-myoc}$ ($r=0.56$; $p=0.06$).

Discussion

We report here that quantitative analysis of myocardial enhancement of patients with CA exhibits significant differences compared with control patients: (1) On first-pass images, the myocardial signal-to-noise ratio (SNR_{myoc}) of the patients with CA was significantly lower than that of the control subjects. (2) On delayed images, the patients with CA exhibited a significantly higher myocardial attenuation and myocardial SNR (SNR_{myoc}), and less difference in contrast between myocardium and blood pool ($CNR_{blood-myoc}$). (3) The variation of myocardial attenuation between delayed and first-pass acquisitions was positive for the patients with CA and negative for the control patients. Qualitative analysis of CT images would appear to be less accurate than quantitative measurements to detect or rule out cardiac amyloidosis.

Table 4 Myocardial and blood pool attenuation, SNR_{myoc} , SNR_{blood} , $CNR_{blood-myoc}$ and relative attenuation index (RAI) in the 13 patients with cardiac amyloidosis and in the 11 control patients on delayed CT images

	Patients with cardiac amyloidosis	Control patients	<i>P</i> value
Myocardial attenuation (HU)	121±39	81±17	0.005
Blood pool attenuation (HU)	148±42	129±33	0.2
SNR_{myoc}	7.10±2.7	5.03±1.8	0.04
SNR_{blood}	8.62±3.0	7.89±2.9	0.5
$CNR_{blood-myoc}$	1.51±0.7	2.85±1.2	0.004
RAI	0.12±0.25	-0.56±0.21	0.04

Data are mean±SD

HU Hounsfield unit

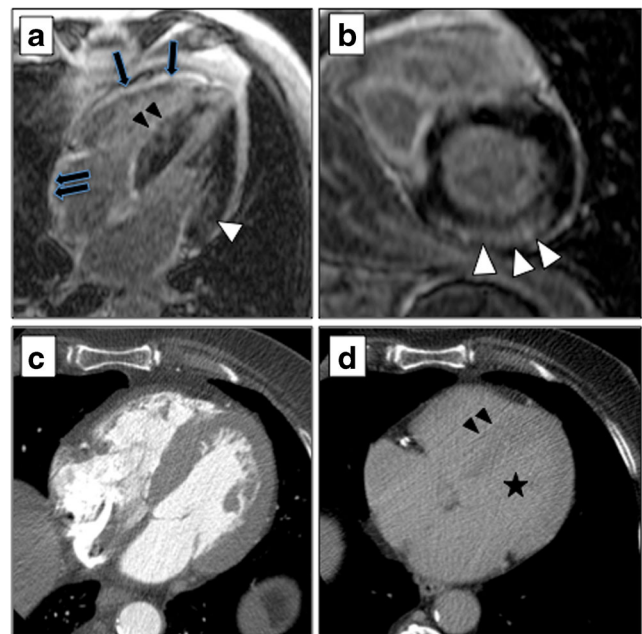


Fig. 1 LGE MR images acquired in the four chamber (a) and in the short axis (b) planes showed heterogeneous myocardial enhancement of the left ventricle (arrowheads), right ventricle (arrows) and atria (double arrow) in one patient with CA. First-pass MDCT images (c) of the patient evidenced a global left ventricular thickening. On delayed MDCT images (d) a reduction of contrast between interventricular septum (arrowheads) and left ventricular blood (star) was detected. The myocardial SNRs were 3.3 and 11.5, respectively, for the first-pass and the delayed acquisition. The relative attenuation index was positive (0.28)

Several studies have evaluated the performance of delayed MDCT in detecting myocardial infarction [11–13], acute myocarditis [17] and fibrosis [16], but to the best of our knowledge none have evaluated myocardial enhancement in patients with CA. CA occurs following interstitial deposit of amyloid proteins resulting in an enlargement of the extracellular space [18, 19]. Gadolinium chelates are non-specific contrast agents that concentrate in the extravascular space [20, 21]. Their accumulation within the enlarged extracellular space of amyloid myocardium has been reported to be the main reason explaining LGE observed on MRI in cardiac amyloidosis [22]. Similarly, iodinated contrast agents are non-specific contrast agents that diffuse in the extracellular space after intravascular injection [23]. As reported by Gerber et al. [12] in a study comparing delayed MDCT and MRI aspects of myocardial infarcts in animals, gadolinium chelates and iodinated contrast agents have similar pharmacokinetic behaviour and distribution volume. We therefore assume that the high myocardial attenuation that we observed on delayed MDCT images in the patients with CA was most probably due to an accumulation of iodinated molecules in the enlarged extracellular space volume of the amyloid heart as for gadolinium chelates on MRI.

On delayed acquisition, the myocardial attenuation of patients was increased in patients with CA and was associated

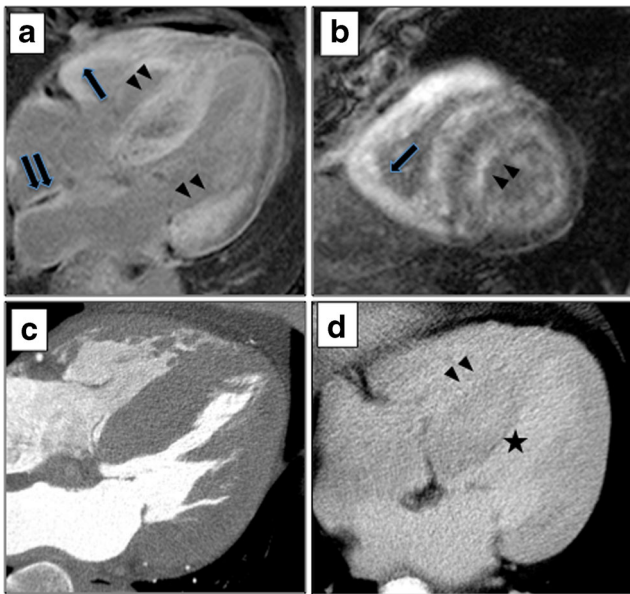


Fig. 2 Another example of diffuse myocardial enhancement of the left ventricle (*arrowheads*), right ventricle (*arrows*) and atria (*double arrow*) associated with diffuse thickening of cardiac wall detected on four chamber (**a**) and short axis (**b**) LGE images in one patient with CA. A thickening of the left ventricular wall was detected on visual analysis of first-pass MDCT images (**c**). On delayed MDCT images a low contrast between interventricular septum (*arrowheads*) and blood pool (*star*) was observed. The myocardial SNRs were 2.7 and 11.4, respectively, for the first-pass and the delayed acquisition. The relative attenuation index was positive (0.30). Note that the patient with CA also exhibited a thickening of the right ventricular wall and the interatrial septum

with a reduction in contrast between blood pool and myocardium ($CNR_{\text{blood-myoc}}$). This could be of interest to identify an infiltrative disease within the myocardium. In contrast, we found that the myocardial attenuation of patients with CA tended to be lower than in control subjects on first-pass images. This suggests that accumulation of iodinated contrast agent within the amyloid myocardium is a progressive phenomenon and it takes a while to fill the increased extracellular volume space. This would explain why we found less enhancement of the myocardium on first-pass images in patients with CV compared with control subjects. The negative correlation that we found between LV wall thickness and first-pass myocardial enhancement reinforces this hypothesis: the greater the cardiac thickness, the longer the myocardium enhancement time. Interestingly, we noticed that patients with CA and control patients exhibited opposite variations of myocardial attenuation between MDCT acquisitions: myocardial attenuation increased between first-pass and delayed acquisitions in patients with CA in contrast to control patients in whom attenuation decreased. These differences reflect modifications of the kinetics of the iodine agent. Thus, we hypothesize that a combined index including both first-pass and delayed myocardial indices—the relative myocardial attenuation index—could be of interest to identify patients with CA.

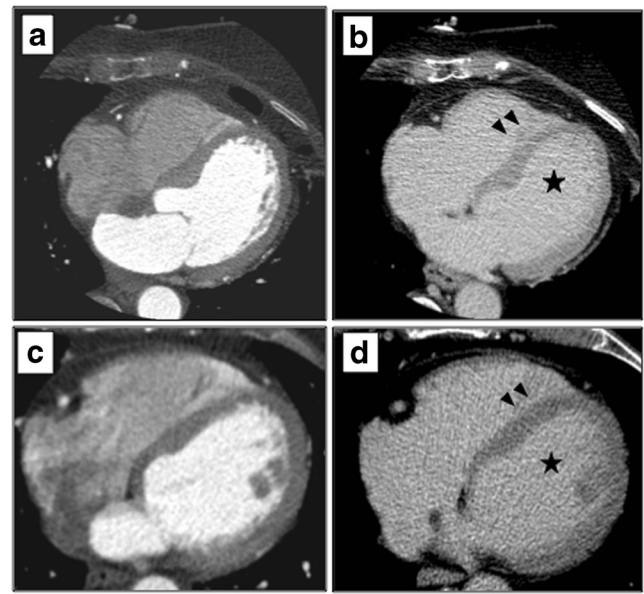


Fig. 3 Examples of first-pass (**a, c**) and delayed (**b, d**) MDCT images of two control patients (*top row* patient 1, *bottom row* patient 2). The control patients had higher first-pass myocardial SNR (6.7 and 5.9, respectively, for patients 1 and 2) than patients with CA presented in Figs. 1 and 2. In contrast, delayed myocardial SNRs of control patients were lower (5.4 and 3.9, respectively, for patient 1 and 2) than patients with CA presented in Figs. 1 and 2. Both control patients had a negative relative attenuation index (−0.86 and −0.50, respectively, for patient 1 and 2). On delayed MDCT images (**b, d**), note the relatively good contrast between interventricular septum (*arrowheads*) and blood (*star*) compared with patients with CA presented in Figs. 1 and 2

Qualitative analysis of CT images showed that the diagnosis of CA was difficult to rule out in a significant number of cases. In addition, qualitative analysis was not sensitive enough to detect CA and a number of patients (31 %) were ranked as doubtful despite a control group that did not exhibit significant thickening of the cardiac wall. It is likely that the detection of subjects with CA would have been lower if the control group had included patients with other causes of hypertrophic left ventricular wall. Comparison of MR and CT images of patients with CA revealed a higher frequency of atria involvement on MR images than on CT images. Despite the possibility of false positive cases on MR images, such data are not surprising and suggest that MRI is more accurate than CT because of its higher signal resolution.

Our study had several limitations which deserve to be mentioned. First of all, the number of included patients was low and our results should thus be interpreted with caution. Further studies with a larger population are needed to confirm these preliminary results. Second, all included patients with CA had a typical CA with left ventricular thickening and diffuse myocardium enhancement. We did not evaluate other MR aspects of CA with subendocardial or a focal enhancement that have been previously described [5, 7]. Thirdly, other causes of left ventricular hypertrophy such as systemic hypertension or valvular disease with potential modification of myocardial attenuation (for instance

because of fibrosis) were not evaluated. Furthermore, delayed acquisition was measured after a 5-min interval as previously reported [24], but other authors have used a 10-min interval for delayed acquisition [12]. In the same way, we did not use a low setting of tube voltage (80 kV) on delayed acquisition, as usually performed, in order to be able to compare myocardial attenuation between first-pass and delayed acquisitions. Finally, although we did not use dual source or multispectral techniques that can improve the differentiation of attenuation between structures using low kV images [25], this could have been of interest in our study.

Conclusion

Myocardial signal-to-noise ratio in our patients with CA was lower on first-pass MDCT acquisition and higher on delayed MDCT acquisition compared with control patients. Mean percentage of variation of myocardial attenuation between delayed and first-pass MDCT acquisitions was positive in patients with CA and negative in control patients. Qualitative analysis would appear to be less accurate than quantitative parameters to detect CA. All in all, our results suggest that quantitative MDCT measurements could be of interest in the detection of CA.

Acknowledgements The scientific guarantor of this publication is Jean-François Deux. The authors of this manuscript declare no relationships with any companies whose products or services may be related to the subject matter of the article. The authors state that this work has not received any funding. One of the authors has significant statistical expertise. Institutional review board approval was obtained. Written informed consent was obtained from all subjects (patients) in this study. Methodology: prospective, experimental, performed at one institution.

References

- Falk RH, Comenzo RL, Skinner M (1997) The systemic amyloidoses. *N Engl J Med* 337:898–909
- Koyama J, Falk RH (2010) Prognostic significance of strain Doppler imaging in light-chain amyloidosis. *JACC Cardiovasc Imaging* 3:333–342
- Selvanayagam JB, Hawkins PN, Paul B, Myerson SG, Neubauer S (2007) Evaluation and management of the cardiac amyloidosis. *J Am Coll Cardiol* 50:2101–2110
- Austin BA, Tang WH, Rodriguez ER et al (2009) Delayed hyper-enhancement magnetic resonance imaging provides incremental diagnostic and prognostic utility in suspected cardiac amyloidosis. *JACC Cardiovasc Imaging* 2:1369–1377
- Maceira AM, Joshi J, Prasad SK et al (2005) Cardiovascular magnetic resonance in cardiac amyloidosis. *Circulation* 111:186–193
- Maceira AM, Prasad SK, Hawkins PN, Roughton M, Pennell DJ (2008) Cardiovascular magnetic resonance and prognosis in cardiac amyloidosis. *J Cardiovasc Magn Reson* 10:54
- Syed IS, Glockner JF, Feng D et al (2010) Role of cardiac magnetic resonance imaging in the detection of cardiac amyloidosis. *JACC Cardiovasc Imaging* 3:155–164
- Vogelsberg H, Mahrholdt H, Deluigi CC et al (2008) Cardiovascular magnetic resonance in clinically suspected cardiac amyloidosis: noninvasive imaging compared to endomyocardial biopsy. *J Am Coll Cardiol* 51:1022–1030
- Mark DB, Berman DS, Budoff MJ et al (2010) ACCF/ACR/AHA/NASCI/SAIP/SCAI/SCCT 2010 expert consensus document on coronary computed tomographic angiography: a report of the American College of Cardiology Foundation Task Force on Expert Consensus Documents. *J Am Coll Cardiol* 55:2663–2699
- Montalescot G, Sechtem U, Achenbach S et al (2013) 2013 ESC guidelines on the management of stable coronary artery disease: the task force on the management of stable coronary artery disease of the European Society of Cardiology. *Eur Heart J* 34:2949–3003
- Baks T, Cademartiri F, Moelker AD et al (2007) Assessment of acute reperfused myocardial infarction with delayed enhancement 64-MDCT. *AJR Am J Roentgenol* 188:W135–W137
- Gerber BL, Belge B, Legros GJ et al (2006) Characterization of acute and chronic myocardial infarcts by multidetector computed tomography: comparison with contrast-enhanced magnetic resonance. *Circulation* 113:823–833
- Nieman K, Shapiro MD, Ferencik M et al (2008) Reperfused myocardial infarction: contrast-enhanced 64-Section CT in comparison to MR imaging. *Radiology* 247:49–56
- Rodriguez-Granillo GA, Rosales MA, Baum S et al (2009) Early assessment of myocardial viability by the use of delayed enhancement computed tomography after primary percutaneous coronary intervention. *JACC Cardiovasc Imaging* 2:1072–1081
- Sato A, Nozato T, Hikita H et al (2012) Prognostic value of myocardial contrast delayed enhancement with 64-slice multidetector computed tomography after acute myocardial infarction. *J Am Coll Cardiol* 59:730–738
- Zhao L, Ma X, Delano MC et al (2013) Assessment of myocardial fibrosis and coronary arteries in hypertrophic cardiomyopathy using combined arterial and delayed enhanced CT: comparison with MR and coronary angiography. *Eur Radiol* 23:1034–1043
- Dambrin G, Laissy JP, Serfaty JM, Caussin C, Lancelin B, Paul JF (2007) Diagnostic value of ECG-gated multidetector computed tomography in the early phase of suspected acute myocarditis. A preliminary comparative study with cardiac MRI. *Eur Radiol* 17:331–338
- Bandula S, Banyersad SM, Sado D et al (2013) Measurement of tissue interstitial volume in healthy patients and those with amyloidosis with equilibrium contrast-enhanced MR imaging. *Radiology* 268:858–864
- Banyersad SM, Sado DM, Flett AS et al (2013) Quantification of myocardial extracellular volume fraction in systemic AL amyloidosis: an equilibrium contrast cardiovascular magnetic resonance study. *Circ Cardiovasc Imaging* 6:34–39
- Canet EP, Janier MF, Revel D (1999) Magnetic resonance perfusion imaging in ischemic heart disease. *J Magn Reson Imaging* 10:423–433
- Weinmann HJ, Brasch RC, Press WR, Wesbey GE (1984) Characteristics of gadolinium-DTPA complex: a potential NMR contrast agent. *AJR Am J Roentgenol* 142:619–624
- Mahrholdt H, Wagner A, Judd RM, Sechtem U, Kim RJ (2005) Delayed enhancement cardiovascular magnetic resonance assessment of non-ischaemic cardiomyopathies. *Eur Heart J* 26:1461–1474
- Bourin M, Jolliet P, Ballereau F (1997) An overview of the clinical pharmacokinetics of x-ray contrast media. *Clin Pharmacokinet* 32:180–193
- Paul JF, Wartski M, Caussin C et al (2005) Late defect on delayed contrast-enhanced multi-detector row CT scans in the prediction of SPECT infarct size after reperfused acute myocardial infarction: initial experience. *Radiology* 236:485–489
- Kartje JK, Schmidt B, Bruners P, Mahnken AH (2013) Dual energy CT with nonlinear image blending improves visualization of delayed myocardial contrast enhancement in acute myocardial infarction. *Invest Radiol* 48:41–45